

Letter

Electronically controlled generation of laser pulse patterns in a synchronously pumped mode-locked semiconductor optical amplifier-fiber laser

Boris Nyushkov^{1,2}, Aleksey Ivanenko¹, Sergey Smirnov¹
and Sergey Kobtsev¹

¹ Novosibirsk State University, Novosibirsk 630090, Russia

² Novosibirsk State Technical University, Novosibirsk 630073, Russia

E-mail: borisn@ngs.ru and ivanenko.aleksey@gmail.com

Received 8 August 2019

Accepted for publication 15 October 2019


Published 31 October 2019



Abstract

A method for electronically controlled formation of user-defined laser pulse patterns in a synchronously pumped laser based on a semiconductor optical amplifier and an all-fiber resonator is proposed and investigated. It is demonstrated that synchronous pumping allows mode-locked operation with the laser radiation structured as an arbitrary pulse pattern repeatable on each cavity round trip. Direct electronic control of the structure and shape of the generated laser pulse patterns is implemented. The accuracy of the reproduction of modulation pulse patterns and waveforms delivered from a radiofrequency arbitrary waveform generator is examined. The time constraint on the pulse pattern formation in the steady-state mode-locked lasing regime is revealed, as well as the feasibility of the quasi-steady-state regime with on-the-lasing continuous modification of the pulse pattern structure.

Keywords: fibre lasers, mode locking, laser radiation characteristics

 Supplementary material for this article is available [online](#)

(Some figures may appear in colour only in the online journal)

1. Introduction

Active mode locking of lasers is the well-established method for obtaining a regular train of relatively short laser pulses whose parameters strongly correlate with the corresponding parameters of a driving electrical signal [1–4]. This method is often implemented by applying intracavity modulation of either the frequency or amplitude. Sufficiently fast modulation allows harmonic mode-locked operation with the possibility for electronically controlled switching of the pulse repetition rate between different high-order harmonics of the fundamental pulse repetition rate as demonstrated in various solid-state

lasers, including fiber-based lasers [5–10]. The inherently strong relationship between the parameters of the modulating electrical signal and the generated laser pulses is also used for implementation of regenerative feedbacks [11–13], stabilization of the laser pulse train against a reference radiofrequency oscillator [14], control of laser pulse duration [15], and dispersion-based wavelength tuning [16, 17]. Nevertheless, the potentialities of direct electronic control over the shape and time structure of the laser pulses in actively mode-locked lasers have not been fully explored. At the same time, lasing in the form of arbitrary-shaped periodic pulse patterns and waveforms is a prospective subject of great interest to both

scientific and industrial communities. Earlier, pulse-periodic lasing regimes with an intrinsically complex structure of generated pulses were investigated in passively mode-locked fiber lasers, namely regimes of double-scale pulses [18], soliton molecules [19], and soliton pattern complexes [20]. However, the methods of such generation are not universal and reliable because their potential to control pulse shape and structure is very limited and dependent on many adjustable and nonadjustable parameters of these lasers.

In the present work, we propose and study an original method for electronically controlled formation of user-defined pulse patterns in an actively mode-locked fiber-cavity laser. This method allows the laser to produce an accurate light replica of the shape and structure of the driving pulse-periodic electrical signal in proper mode-locked lasing conditions. This opens up possibilities for direct laser generation of user-specified periodic pulse patterns composed of nearly-arbitrary-shaped pulse elements or waveforms. The aforesaid method was implemented and studied in a hybrid semiconductor optical amplifier (SOA)-fiber laser, whose mode-locked operation was forced by synchronous electrical pumping of the SOA. Synchronous pumping is the energy-efficient approach to active mode locking in different types of modulator-free lasers [21–23]. An early implementation of a synchronously pumped hybrid SOA-fiber laser allowed switchable harmonic mode locking with a high (sub-GHz) pulse repetition rate [24]. A later work [25] proved the feasibility of ultra-long synchronously pumped SOA-fiber lasers with a kilohertz-scale fundamental pulse repetition rate. It also suggested the further investigation of electronic control over laser pulse shaping by manipulation of the pumping electrical pulses. We suppose, however, that such control is subject to the conditions of steady-state mode-locked laser action, and can also be affected by optical nonlinearity and dispersion in the SOA-fiber lasers. Earlier, ultrashort pulse shaping in passively mode-locked fiber lasers was shown to be greatly dependent on the interplay and distribution of dispersion, nonlinearity, gain, and energy dissipation within the fiber cavity [26]. Therefore, to avoid complex nonlinear distortions, we investigate here the feasibility of the proposed method of forced pulse shaping and patterning in conditions of negligible optical nonlinearity and dispersion. Mode-locked pulse patterning is examined within the (sub)microsecond time scale, thus ensuring relatively low peak power and a narrow optical spectrum.

2. Experimental

The experimental set-up is schematically shown in figure 1. The laser cavity has an all-fiber ring-linear configuration composed of a fiber-coupled SOA, a 50% output fiber coupler, and a fiber circulator ensuring unidirectional lasing in the ring part of the cavity. This circulator also forms the linear arm of the cavity, where a fiber Bragg grating (FBG, produced by the Institute of Automation and Electrometry SB RAS) is installed for lasing wavelength selection and stabilization. The reflection spectrum of the used FBG is approximately 1 nm wide and centered at ~ 1540 nm, and its reflection coefficient is

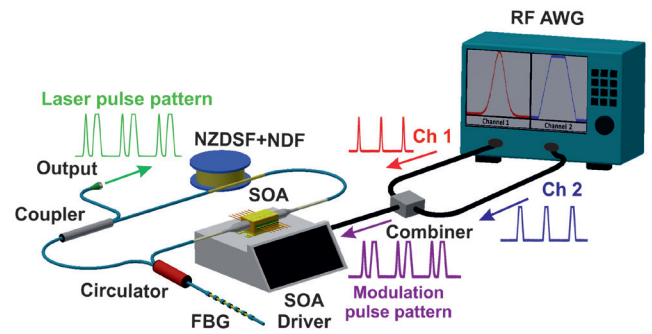


Figure 1. The synchronously pumped SOA-fiber laser with electronic control of pulse patterning: SOA—semiconductor optical amplifier, NDF—normal-dispersion fiber, NZDSF—non-zero dispersion shifted fiber, FBG—fiber Bragg grating, RF AWG—radiofrequency arbitrary waveform generator, Ch1, Ch2—channels 1 and 2.

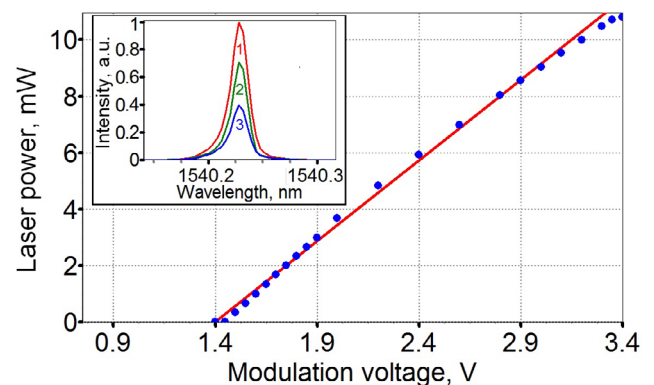


Figure 2. Transfer characteristics of the modulation input of the SOA-fiber laser (CW lasing power versus applied direct voltage). The blue circles mark the measured dependence; the red straight line represents its linear fitting. Inset: the laser optical spectra acquired at different voltages (#1—at 2.6 V, #2—at 2.2 V, #3—at 1.8 V).

~ 0.95 . The ring part of the cavity is extended by spliced pieces of a 2.4 km long normal-dispersion fiber (Corning MetroCor) and a 2.4 km long non-zero dispersion shifted fiber (True-Wave Classic). The latter has anomalous dispersion at the lasing wavelength.

The designed ultra-long cavity features a quite low (43.35 kHz) intermode frequency. This relaxes the speed requirements of the SOA current controller, which has to be modulated at the cavity intermode frequency or its multiple, and also allows enhancement of per-pulse energy in the single-pulse mode-locked lasing regime. The SOA (Thorlabs SOA 1013S) was pumped electrically through a current driver modulated by user-defined electrical pulse patterns. These control pulse patterns were formed by means of a programmable dual-channel radiofrequency arbitrary waveform generator (RF AWG) Rigol DG4162, based on the technology of direct digital synthesis. The combined signal from the AWG outputs was sent to the modulation input of the SOA driver to manage synchronous pumping of the laser. The laser characteristics were measured by using a power meter, an optical spectrum analyzer (OSA), and a couple of fast photodiodes connected to an oscilloscope and RF spectrum analyzer.

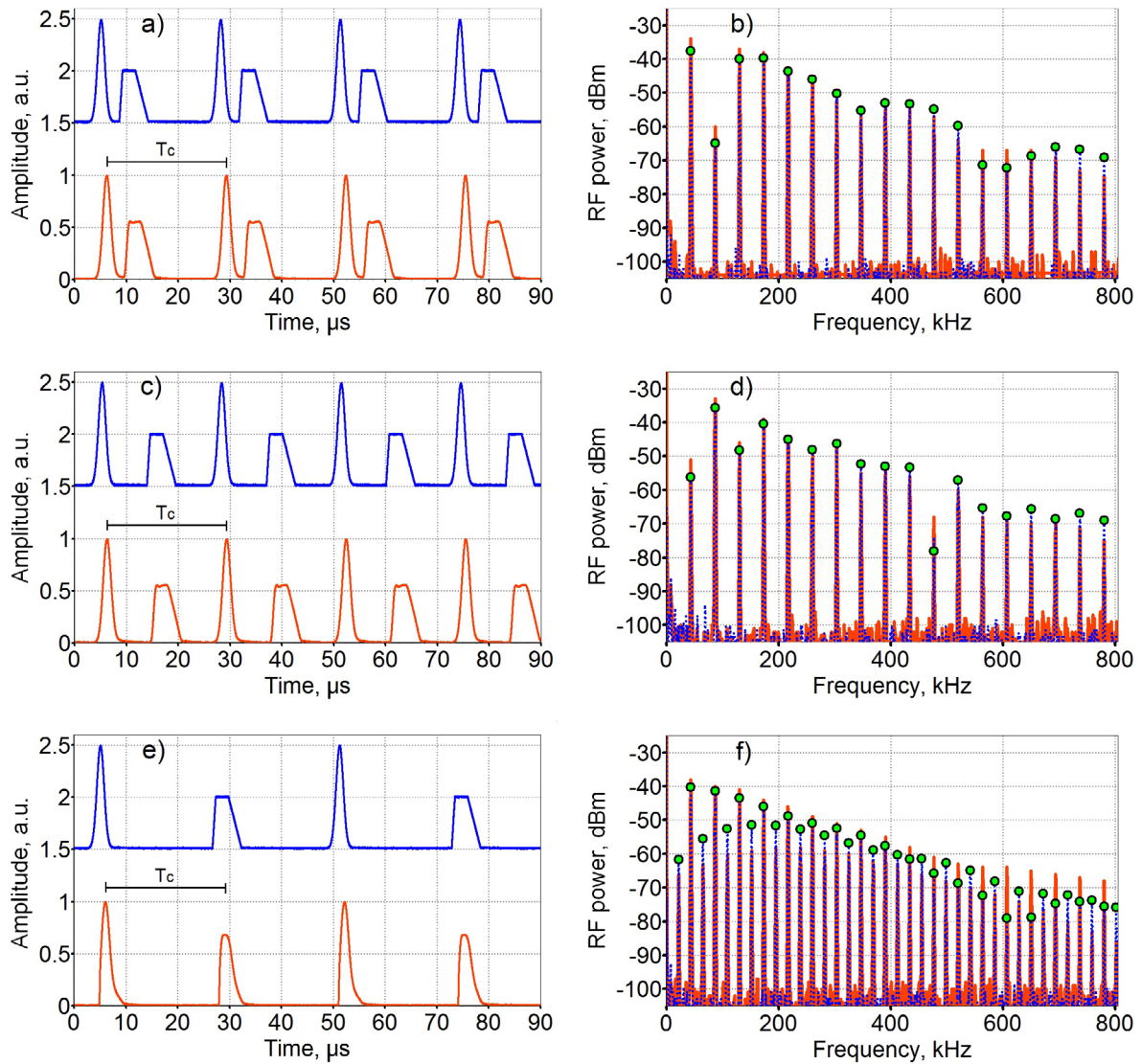


Figure 3. Oscillograms (a), (c), (e) and the corresponding RF spectra (b), (d), (f) measured for both modulation pulse patterns (blue) and laser pulse patterns (red). Note: green circles indicate the theoretical RF spectra; the frequency spacing in the RF spectra (b) and (d) is 43.35 kHz, while the frequency spacing in the RF spectra (f) is 21.675 kHz; the resolution bandwidth (RBW) is 1 kHz; T_c is the cavity round-trip time.

3. Results and discussion

First, we measured the transfer characteristics of the laser modulation input in the continuous-wave (CW) regime in order to define the appropriate dynamic range for the synchronous pumping regime. The plot in figure 2 represents the revealed dependence of the laser output power on the voltage applied to the modulation input of the SOA driver. The threshold voltage for lasing was found to be about 1.47 V. The cutoff voltage corresponding to the maximum current allowable for the SOA was 3.38 V. The laser power reached 10.8 mW at the maximum voltage. It is noticeable that the measured characteristic can be well fitted with a linear function. This suggests that the modulation-based laser pulse shaping can be free of significant nonlinear distortions. Simultaneous monitoring of laser radiation using the OSA revealed the stability of the lasing wavelength against the modulation voltage variation

(as shown in the inset in figure 2), which was defined with an accuracy limited by the OSA resolution (0.02 nm).

On this basis, for the pulsed lasing exploration we set the lower limit of the modulation voltage at 1.55 V, which is slightly above the lasing threshold. This prevents the lasing dynamics from transient processes related to overcoming of the threshold. The upper limit of the modulation voltage was set at 3.1 V. Such laser gain control can be referred to as gain modulation, rather than gain switching [27]. The modulation depth derived from the corresponding dynamic range of the laser power was about 93%.

A regular train of a user-defined electrical pulse pattern with the amplitude corresponding to the above-stated voltage range was delivered from the AWG to the modulation input of the laser. The repetition frequency of the modulation pulse pattern was set at 43.35 kHz to match the cavity round-trip time ($T_c = 23.1 \mu\text{s}$) of the pulsed laser radiation. This

frequency also corresponds to the frequency spacing between adjacent longitudinal modes in the laser cavity (the intermode frequency) at the lasing wavelength. Thus, the synchronously pumped mode-locked lasing with the radiation structured and shaped as a replica of the modulation (i.e. pumping) pulse pattern was obtained.

To characterize the accuracy of the reproduction of a reference pulse pattern by the laser, we measured and compared the RF spectra of a modulation pulse pattern train and the corresponding laser pulse pattern train. We evaluated the discrepancies between these spectra as well as between them and the theoretical spectrum derived from Fourier transform of the original mathematical function used to describe the pulse pattern in the AWG.

Initially, the synchronous pumping was performed with the electrical pulse pattern composed of a Gaussian and an asymmetric trapezoid (as shown in figure 3(a)). These elements differed in amplitude and were allocated within the time span corresponding to the cavity round trip time T_c . The pattern elements were formed separately in the synchronized AWG channels and then combined into the whole pattern before the modulation input of the laser. This allowed optional altering of the time delay between the pattern elements. Figure 3 represents the laser characteristics obtained when applying the described modulation pulse pattern to synchronous pumping.

The oscillograms shown in figures 3(a) and (c) evidence the capability of the laser to reproduce modulation pulse patterns with different time intervals between the pattern elements, provided that the repetition period of the whole pulse pattern equals the cavity round-trip time ($T_{\text{pattern}} = T_c$). The corresponding RF spectra of the modulation pulse pattern trains and laser pulse pattern trains are shown in figures 3(b) and (d). These spectra allow one to evaluate how accurately the amplitude–frequency characteristics of the modulation pulse patterns are reproduced by the laser. Also, the RF spectra of the laser radiation allow verification of the mode-locked nature of the obtained lasing regime. The observed stable comb-like structure of the RF spectra featured the frequency spacing equal to the laser intermode frequency and the relatively high (up to 60 dB) signal-to-noise ratio of individual spectral components. These features are typically indicative of the mode-locked lasing regime. The reproduction accuracy of the RF spectral characteristics was evaluated over the frequency band 0.01–0.8 MHz, which is adequate for both the microsecond time scale of the pulse patterns and for the kilohertz-scale intermode frequency of the laser cavity. The least-squares procedure was used for appropriate fitting of the spectral amplitudes of the modulation pulse patterns to the spectral amplitudes of corresponding laser pulse patterns when superposing the RF spectra for comparison (as shown in figure 3). The root-mean-square discrepancy (RMSD) between the spectral amplitudes of the modulation and laser pulse patterns was then evaluated as an integral criterion of accuracy of the pulse pattern reproduction in the frequency domain. But first, we found an RMSD between the theoretical and measured RF spectra of the modulation pulse pattern. It did not exceed 1.2 dB for the above described pulse patterns. This RMSD value characterizes how accurately the original



Figure 4. Captured video of on-the-lasing continuous modification of the laser pulse pattern structure. The instrumentation displayed left-to-right: an RF spectrum analyzer measuring the RF spectrum of the laser pulse pattern train, a digital oscilloscope measuring the modulation pulse pattern train (upper oscillogram) and the corresponding laser pulse pattern train (lower oscillogram), and a dual-channel RF AWG forming the modulation pulse pattern train. The inset indicates the repetition frequencies set for each AWG channel.

mathematical function used to describe the pulse pattern was reproduced by the AWG when forming the modulation pulse pattern. At the same time, the RMSD between the measured RF spectra of the modulation pulse patterns and resulting laser pulse patterns did not exceed 3.4 dB.

It is also important to note that the observed RF spectrum of the above two-element pulse pattern features significant relative variations (up to 20 dB) in its spectral amplitudes when changing the time interval between its constituent elements. It is clearly seen when looking at and comparing the RF spectra presented in figures 3(b) and (d).

In this connection, it was interesting for us to examine the possibility of on-the-lasing dynamic modification of the pulse pattern structure. To this end, we introduced a slight frequency detuning (0.2 Hz) between the AWG channels used to compose the modulation pulse pattern. This enabled cyclic variation of the time interval between the constituent elements of the pulse pattern with a sweep time of 5 s. The laser pulse pattern under these conditions was repeating both the shape and dynamics of the modulation pulse pattern, as presented on the captured video (stacks.iop.org/LPL/16/115103/mmedia) (figure 4). Such a lasing regime can be considered as a quasi-steady-state regime on the condition that the pulse pattern modification rate is very slow in comparison with the cavity round-trip time.

The time constraint on the pulse pattern formation in the steady-state mode-locked lasing regime was revealed experimentally as well, namely the requirement for appropriate pulse pattern timing for precise matching with the cavity round-trip time. Thus, upon doubling of the modulation pulse pattern period ($T_{\text{pattern}} = 2T_c$), the laser could not reproduce the shape of the pulse pattern elements as accurately as in the above described cases, despite the fact that the elements of the modulation pattern remained the same, and the time interval between them was equal to T_c (figure 3(e)). The laser tended to ‘averaging’ of the shapes of the pulse pattern elements due to alternation of the time profile of the laser gain every other cavity round trip. Such a lasing regime was not

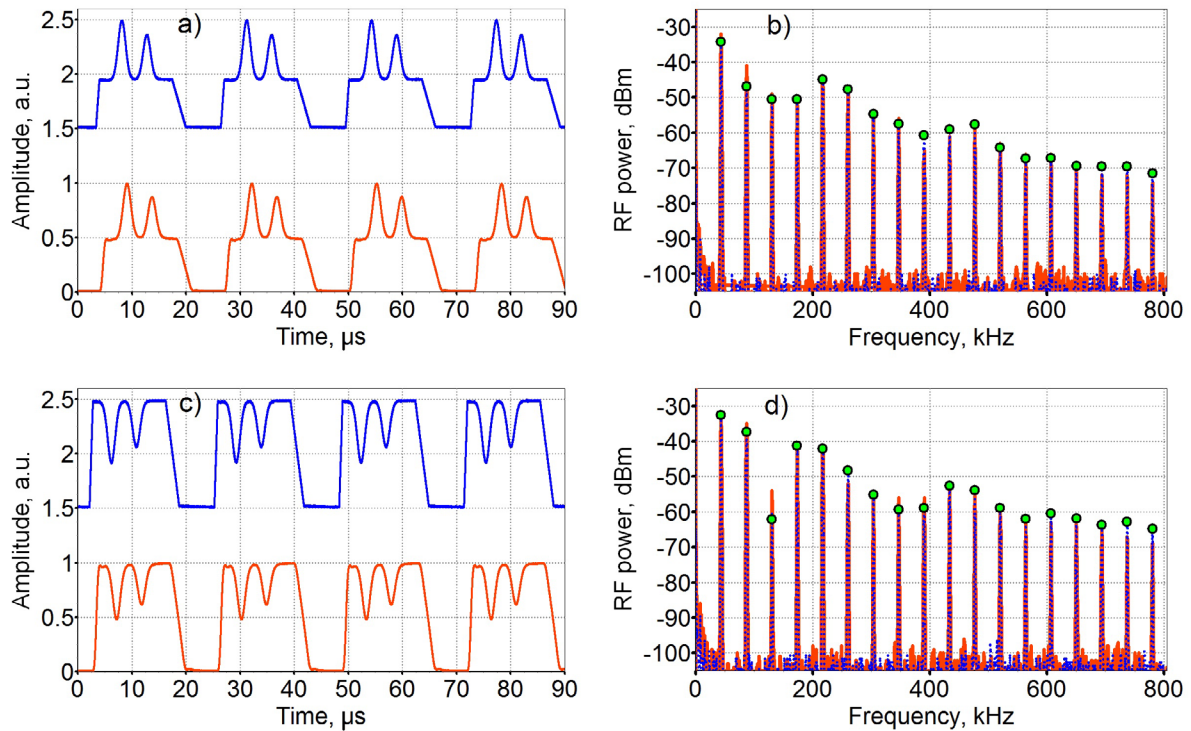


Figure 5. Oscillograms (a), (c) and the corresponding RF spectra (b), (d) measured for both modulation pulse patterns (blue) and laser pulse patterns (red). Note: green circles indicate the theoretical RF spectra; the frequency spacing in all RF spectra is 43.35 kHz; RBW = 1 kHz.

inherently steady-state. In this regime, the pulse pattern trains featured equidistant comb-like RF spectra (figure 3(f)) with a frequency spacing of 21.675 kHz, which is half of the laser intermode frequency defined by the laser cavity length. In this instance the RMSD between the measured RF spectra of the modulation pulse patterns and corresponding laser pulse patterns became as large as 6.2 dB.

Apparently pulse patterns can have a more complex structure than just two discrete elements within the repetition period. We also tested the applicability of the proposed method for generation of arbitrary-shaped periodic waveforms. Figures 5(a)–(d) represent the laser characteristics obtained when applying some specific waveforms to synchronous pumping. The duty cycle of these waveforms amounted to approximately 74%. Measurements and comparison of the corresponding RF spectra (the modulation waveform train against the laser waveform train) revealed that the waveform reproduction accuracy and mode locking quality are no worse than that of the initial two-element pulse pattern. The analyzed spectra are presented in figures 5(b) and (d). The RMSD between the measured RF spectra of the modulation waveforms and corresponding laser spectra did not exceed 2.5 dB over the given frequency band, while the RMSD between the theoretical and measured RF spectra of the modulation waveforms did not exceed 0.8 dB.

It is also important to note that the optical spectra measured during generation of the above described pulse patterns and waveforms were stably centered at the same wavelength

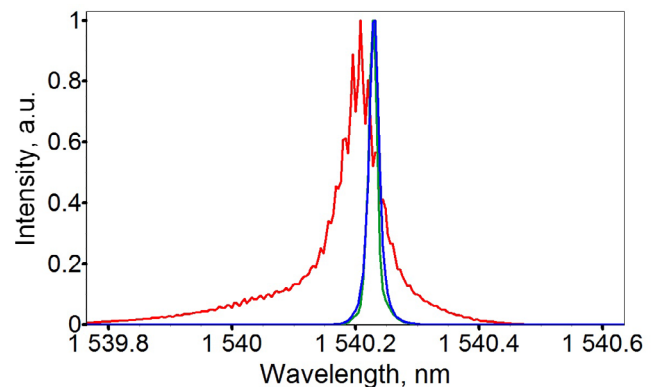


Figure 6. The laser optical spectra acquired under different conditions of pulse pattern generation. The narrow spectra plotted in blue and green are typical of the patterns shown in figures 3 and 5, respectively, provided that the repetition period of the whole pulse pattern equals the cavity round-trip time ($T_{\text{pattern}} = T_c$). The wider spectrum plotted in red corresponds to an attempt to double the pulse pattern period ($T_{\text{pattern}} = 2T_c$), as shown in figure 3(e).

as during CW lasing (~ 1540.2 nm). The measured spectra featured nearly equal widths defined mostly by the moderate spectral resolution (0.02 nm) provided by the OSA. Therefore, they were hardly distinguishable from the spectra measured during CW lasing (inset in figure 2). The exception was only the spectrum acquired during an attempt to double the pulse pattern period ($T_{\text{pattern}} = 2T_c$, as shown in figure 3(e)). This non-steady-state laser operation featured a wider and noisier

optical spectrum affected by amplified spontaneous emission. Figure 6 presents typical optical spectra acquired under different conditions of pulse pattern generation.

Nevertheless, we conclude that the relatively narrow width of the optical spectra prevents generated pulse patterns and waveforms from noticeable dispersion-induced distortions in spite of an ultra-long fiber-based laser cavity.

Relatively linear transfer characteristics of the laser modulation input also make it possible to define the average output laser power without direct measurement of the optical power, even in the case of pulse patterns or waveforms. The calibration plot shown in figure 2 suggests that the output laser power reaches 9.5 mW at the maximal modulation voltage of 3.1 V. During generation of the periodic waveform shown in figure 5(c), the measured average output power amounted to ~6.2 mW. Considering this waveform as an example, one can calculate its integral over the modulation period. It equals 0.65 when normalized to CW lasing at the maximal modulation voltage. Thus, the calculated and measured power-related values are in good agreement. Automatic computation of the average output laser power may be a useful option for the programmable electronic control implemented for generation of user-defined laser pulse patterns and waveforms.

Finally, it should be noted that the nearly 1 μ s temporal resolution limit in the present work is due to the moderate modulation bandwidth of the used SOA current driver. Faster pumping electronics will also allow pulse patterning within the nanosecond time scale. Generation of such relatively long transform-limited pulses in the mode-locked regime is now of emerging interest because of the possibility of being able to fully characterize their spectral properties in the RF domain by using GHz-bandwidth optoelectronics [28].

4. Conclusion

We have demonstrated that mode-locked lasing driven by synchronous pumping can stably sustain nearly arbitrary laser pulse patterns repeatable on each cavity round trip. Electrical synchronous pumping of a hybrid SOA-fiber laser allows implementation of direct electronic control of the structure and shape of the generated laser pulse patterns and waveforms. The accuracy of the laser reproduction of modulation pulse patterns and waveforms has been evaluated as relatively high under conditions of appropriate pulse pattern timing for its precise matching with the cavity round-trip time. Also, we have demonstrated the feasibility of the quasi-steady-state regime with slow on-the-lasing continuous modification of the pulse pattern structure. Considering the nearly 1 ns response time of conventional SOAs, the investigated method of lasing is directly applicable to pulse patterning within nanosecond and microsecond time scales in which dispersion-induced distortions are negligible. Moving in the picosecond time scale will be possible with faster SOAs and careful dispersion management. The most important advantages of the demonstrated direct generation of user-defined laser pulse patterns and waveforms are relative simplicity, compactness, energy-efficiency, and inherent synchronization with an external

clock. We believe that a number of application areas may benefit from these features.

Acknowledgments

The work of AI was supported by the Russian Foundation for Basic Research (Project 18-32-20021). The work of SS was supported by the Ministry of Science and Higher Education of the Russian Federation (Project 3.5572.2017/BCH). The work of SK was supported by the Ministry of Science and Higher Education of the Russian Federation (Project 3.889.2017/PCH).

References

- [1] Kuizenga D and Siegman A 1970 FM and AM mode locking of the homogeneous laser—Part I: theory *IEEE J. Quantum Electron.* **6** 694–708
- [2] Haus H 1975 A theory of forced mode locking *IEEE J. Quantum Electron.* **11** 323–30
- [3] Bowers J E, Morton P A, Mar A and Corzine S W 1989 Actively mode-locked semiconductor lasers *IEEE J. Quantum Electron.* **25** 1426–39
- [4] Haus H A 2000 Mode-locking of lasers *IEEE J. Sel. Top. Quantum Electron.* **6** 1173–85
- [5] Longhi S, Laporta P, Taccheo S and Svelto O 1994 Third-order-harmonic mode locking of a bulk erbium:ytterbium:glass laser at a 2.5 GHz repetition rate *Opt. Lett.* **19** 1985–7
- [6] Yoshida E and Nakazawa M 1996 80–200 GHz erbium doped fibre laser using a rational harmonic mode-locking technique *Electron. Lett.* **32** 1370–2
- [7] Abedin K S, Onodera N and Hyodo M 1999 Higher order FM mode locking for pulse-repetition-rate enhancement in actively mode-locked lasers: theory and experiment *IEEE J. Quantum Electron.* **35** 875–90
- [8] Takara H, Kawanishi S, Saruwatari M and Noguchi K 1992 Generation of highly stable 20 GHz transform-limited optical pulses from actively mode-locked Er³⁺-doped fibre lasers with an all-polarisation maintaining ring cavity *Electron. Lett.* **28** 2095–6
- [9] Carruthers T F and Duling I N 1996 10 GHz, 1.3 ps erbium fiber laser employing soliton pulse shortening *Opt. Lett.* **21** 1927–9
- [10] Bakhshi B and Andrekson P A 2000 40 GHz actively mode-locked polarisation maintaining erbium fibre ring laser *Electron. Lett.* **36** 411–3
- [11] Turi L and Krausz F 1991 Amplitude modulation mode locking of lasers by regenerative feedback *Appl. Phys. Lett.* **58** 810–2
- [12] Bekal A, Vijayan K and Srinivasan B 2015 Characterization of regenerative stabilized actively mode-locked fiber laser incorporating a saturated amplifier in feed-back chain *Opt. Laser Technol.* **67** 98–106
- [13] Nyushkov B N, Ivanenko A V, Kobtsev S M, Pivtsov V S, Farnosov S A, Pokasov P V and Korel I I 2017 Quasi-regenerative mode locking in a compact all-polarisation-maintaining-fibre laser *Quantum Electron.* **47** 1094–8
- [14] Yoshida M, Hirayama T, Nakazawa M, Hagimoto K and Ikegami T 2007 Regeneratively mode-locked fiber laser with a repetition rate stability of 4.9×10^{-15} using a hydrogen maser phase-locked loop *Opt. Lett.* **32** 1827–9
- [15] Chen H, Chen S P, Jiang Z F, Yin K and Hou J 2014 All fiber actively mode-locked ytterbium-doped laser with large

- range temporal tunability *IEEE Photonics Technol. Lett.* **26** 1786–9
- [16] Pan S, Zhao X, Yu W and Lou C 2008 Dispersion-tuned multi-wavelength actively mode-locked fiber laser using a hybrid gain medium *Opt. Laser Technol.* **40** 854–7
- [17] Koliada N A, Nyushkov B N, Ivanenko A V, Kobtsev S M, Harper P, Turitsyn S K and Pivtsov V S 2013 Generation of dissipative solitons in an actively mode-locked ultralong fibre laser *Quantum Electron.* **43** 95–8
- [18] Kobtsev S, Kukarin S, Smirnov S, Turitsyn S and Latkin A 2009 Generation of double-scale femto/pico-second optical lumps in mode-locked fiber lasers *Opt. Express* **17** 20707–13
- [19] Gui L, Wang P, Ding Y, Zhao K, Bao C, Xiao X and Yang C 2018 Soliton molecules and multisoliton states in ultrafast fibre lasers: Intrinsic complexes in dissipative systems *Appl. Sci.* **8** 201
- [20] Amrani F, Salhi M, Grelu P, Leblond H and Sanchez F 2011 Universal soliton pattern formations in passively mode-locked fiber lasers *Opt. Lett.* **36** 1545–7
- [21] AuYeung J C and Johnston A R 1982 Picosecond pulse generation from a synchronously pumped mode-locked semiconductor laser diode *Appl. Phys. Lett.* **40** 112–4
- [22] Peter D S, Beaud P, Hodel W and Weber H P 1991 Passive stabilization of a synchronously pumped mode-locked dye laser with the use of a modified outcoupling mirror *Opt. Lett.* **16** 405–7
- [23] Granados E, Pask H M and Spence D J 2009 Synchronously pumped continuous-wave mode-locked yellow Raman laser at 559 nm *Opt. Express* **17** 569–74
- [24] Pedersen N V, Jakobsen K B and Vaa M 1996 Mode-locked 1.5 μm semiconductor optical amplifier fiber ring *J. Light-wave Technol.* **14** 833–8
- [25] Nyushkov B N, Kobtsev S M, Komarov A K, Komarov K P and Dmitriev A K 2018 SOA fiber laser mode-locked by gain modulation *J. Opt. Soc. Am. B* **35** 2582–7
- [26] Wise F W, Chong A and Renninger W H 2008 High-energy femtosecond fiber lasers based on pulse propagation at normal dispersion *Laser Photonics Rev.* **2** 58–73
- [27] Connelly M 2003 Semiconductor optical amplifiers and their applications *Presented at the Third Spanish Meeting of Optoelectronics, OPTOEL'03 (Madrid, Spain, 14–16 July 2003)*
- [28] Kues M, Reimer C, Wetzel B, Roztocki P, Little B E, Chu S T, Hansson T, Viktorov E A, Moss D J and Morandotti R 2017 Passively mode-locked laser with an ultra-narrow spectral width *Nat. Photon.* **11** 159–62